2nd International Conference on Sustainable Energy Storage, June 19-21, Trinity College Dublin, Ireland

BIPV/T versus BIPV/T-PCM: A numerical investigation of advanced system integrated into SolarXXI building façade

Aelenei, L., Pereira, R., Gonçalves, H.

Energy Efficiency Unit of National Energy and Geology Laboratory, Lisbon Portugal
E-mail : laura.aelenei@lneg.pt

Keywords *: Sustainable Energy Storage, Phase change materials, modeling*

1. INTRODUCTION

Designing energy efficient and affordable solutions integrated in buildings dealing with summer and winter climate challenges present a very ambitious target. In addition to this, in May 2010 the recast of the Directive on Energy Performance of Building [1] set Zero Energy performance targets for all new buildings. The integration of PV systems into buildings becomes imperative in this context.. In the present work the authors of this paper are willing to share a numerical investigation results from on-going research project that pretends to investigate advanced technological prefabricated modules integrating PV and PCM for improving the indoor thermal conditions and reducing building energy demand, through direct electricity generation, solar thermal contributions and energy storage in residential and non-residential buildings [2]. As is well known, only approximately 16% of the solar energy incident on PV converted to electricity, the remaining being absorbed and transformed into heat [3] . At the same time, one major potential problem with PV integrated systems is overheating. Elevated operating temperatures reduce the solar energy conversion efficiency of photovoltaic module. The study will follow two important trends: one is the improving the indoor thermal comfort, reducing at the same time the building energy demands; and second, improving the efficiency of the photovoltaic system by limiting temperature rise inside the system. These two objectives can be achieved by ventilating the air gap behind the PV module, the heat released in the conversion process from PV being successfully recover for indoor heating (BIPV/T) or by using PCM for regularization the temperature difference indoor-outdoor and a rapid stabilization of PV modules temperature (BIPV/T-PCM).

NOMENCLATURE

Cp_{air}	Specific heat of the air [J/(Kg.K)]
Cp_{pv}	Specific heat of the PV [J/(Kg.K)]
Cp_{w}	Specific heat of the isolated brick or PCM [J/(Kg.K)]
$F_{Rpv-pcm}$	View factor between the PV and PCM panes
G	Total incident solar radiation no the plane of the collector per unit area [W/m^2]
h_e	Exterior convective heat transfer coefficient per unit area [W/(m^2.K)]
h_i	Interior convective heat transfer coefficient per unit area [W/(m^2.K)]
h_{pvac}	Convective heat transfer coefficient for the PV/Air Cavity surface per unit area [W/(m^2.K)]
h_r	Cavity radiative heat transfer coefficient per unit area [W/(m^2.K)]
h_r	Radiative heat transfer coefficient between PV and PCM surfaces [W/(m^2.K)]
h_{wac}	Convective heat transfer coefficient for the Air Cavity/Wall surface per unit area [W/(m^2.K)]
L	Latent Heat [J/Kg]
L_p	Latent heat for the temperature rage [J/Kg]
m	Air mass flow rate [Kg/s]
M_{air}	Air cavity thermal mass [Kg]
$\dot{m}_{air}$	Air mass flow [Kg/s]
M_{pv}	PV thermal mass [Kg]
M_w	Wall thermal mass (Isolated Brick or PCM) [Kg]
q_l	Latent heat flux when phase change occurs [W]
R	Heating and cooling rate [°C/s]
R_{pv}	Thermal Resistance of the PV pane [(m^2.K)/W]
R_w	Thermal Resistance of the Wall pane (Isolated Brick or PCM) [(m^2.K)/W]
T_1	Temperature at which the freezing process starts [°C]
T_2	Temperature at which the freezing process ends [°C]
T_{ac}	Average air temperature for the control volume [°C]
T_{dp}	Dew point temperature [°C]
T_{epv}	PV exterior surface temperature of the control volume [°C]
T_{ew}	Brick wall or PCM exterior surface temperature of the control volume [°C]
T_{in}	Room temperature [°C]
T_{inlet}	Inlet air temperature in vents [°C]
T_{ipv}	PV air cavity interior surface temperature of the control volume [°C]
T_{iw}	Brick wall or PCM interior surface temperature of the control volume [°C]
T_{mpv}	PV temperature at the middle of the module at the control volume [°C]
T_{mw}	Brick wall or PCM temperature at the middle of the pane at the control volume [°C]
T_{out}	Ambient air temperature [°C]
T_{outlet}	Outlet air temperature in vents [°C]
T_{sky}	Sky temperature for radiative exchanges [°C]
V_{ch}	Air speed in the channel [m/s]
V_{wind}	Wind velocity [m/s]
α	Solar absorptance
ε_{pcm}	PCM long-wave emissivity
ε_{pv}	PV long-wave emissivity
σ	Stefan-Bolzmann constant

The designing of such a system, however, is a very complex task, for which a scientific investigation (numerical an experimental) of the heat and mass transfer phenomena through the prefabricated module is needed. This paper focus on the first part of the developing project results, a deep analysis of the main processes (convection, radiation, conduction) developing through the module is be done in order to bring out the geometrical and physical features and the ventilation strategies for which the system will be likely to exhibit a maximum thermal and energy efficiency in the Portuguese climatic context.

2. DESCRIPTION OF THE SYSTEMS

The present study has been conducted on two different systems. One of them is a BIPV/T, Building Integrated Photovoltaic with thermal recovery, and the other one is a hybrid integration system integrating PCM, Phase Change Materials and PV. The BIPV-T system is already exists integrating the façade of SolarXXI office building located in Lisbon, Portugal, the other one BIPV-PCM, is already constructed and installed, and is expected that in the near period, the experimental analysis will be performed.

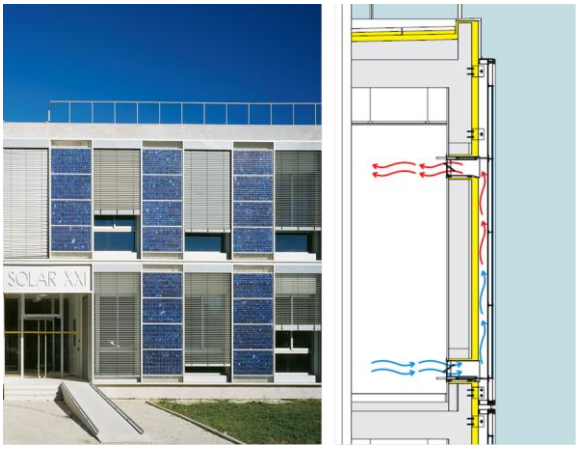

Fig. 1, Solar XXI building façade. BIPV-T

2.1. BIPV/T

The existing BIPV/T system on the SOLAR XXI building consists of a photovoltaic module with 0,04m thickness, an air cavity with 0,16m thickness, isolated brick wall with 0,28m of thickness and two adjustable dampers (Fig. 1). For the winter season the system assumes two different heating configurations as show on Fig. 1. During the day period, the system assumes the ventilated configuration where the vents stays opened, and the air flows by natural convection within air cavity. During night, the system assumes the non-ventilated configuration and the vents stay closed. Both systems have the same configuration, of two opaque layers and an air gap formed between them assuming the same two configurations for the winter season (Fig. 2).

2.2. BIPV/T-PCM

The proposed system, for the winter configuration, consists in the same photovoltaic module and air cavity thicknesses. A PCM board, with 0,013 m thickness, substitutes the isolated brick wall.

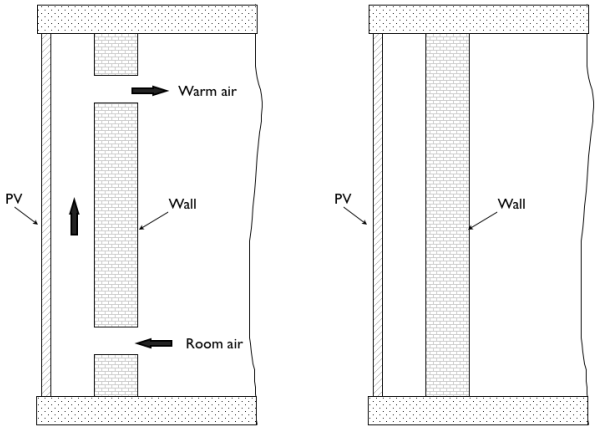

Fig. 2, Ventilated BIPV/T system (left), Non-Ventilated BIPV/T system (right)

3. NUMERICAL SIMULATION MODEL

The dynamic model was simulated using the real climatic data of winter time measured on the building site.

It was used a numerical dynamic simulation model inside the control volume. It means that at every time step, the model requires the solution of the previous time step with a fully finite difference scheme. The programming MATLAB/SIMULINK® with SIMSCAPE® library was used to numerically find the solution of both models. This software has a user-friendly interface and good flexibility. The SIMSCAPE® library permits a very dynamical simulation. Fig. 3 shows the software model interface.

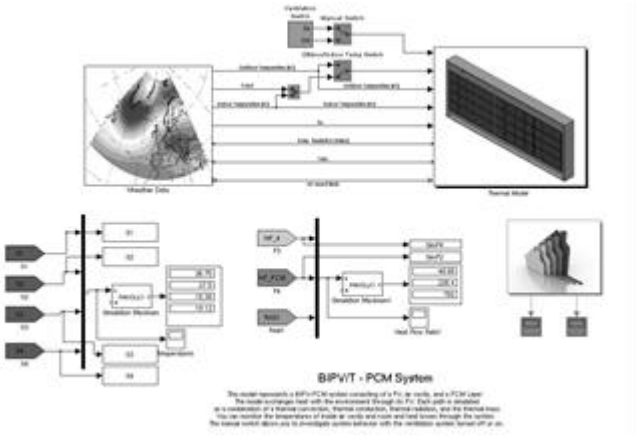

Fig. 3. Software model interface.

3.1. Thermal model. Equations

The BIPV/T and the BIPV/T-PCM models considered here are shown schematically in Fig. 3.

A transversal control volume was set to equalize the PV area.

The two models are identical, differing only in the wall material (Isolated Brick or PCM)

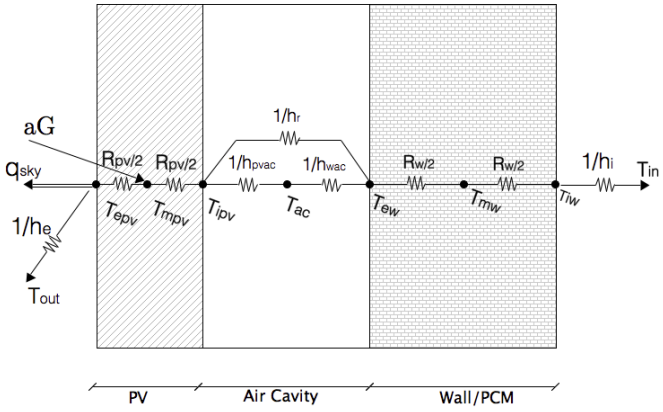

Fig. 4. Model studied – Thermal network

3.1.1. BIPV/T Model

The equations corresponding to a representative control volume in the model (Fig. 4) are show below.
Each equation represents the energy balance to each node of the network.

$$\frac{\left(T_{mpv}-T_{epv}\right)}{R_{pv}/2}-\varepsilon_{pv}\cdot\sigma\cdot\left(T_{epv}^4-T_{sky}^4\right)-h_e\left(T_{epv}-T_{out}\right)=0 \quad (1)$$

$$M_{pv}\cdot Cp_{pv}\cdot\frac{\partial T_{mpv}}{\partial t}=\alpha_{pv}\cdot G+\frac{\left(T_{epv}-T_{mpv}\right)}{R_{pv}/2}-\frac{\left(T_{mpv}-T_{ipv}\right)}{R_{pv}/2} \quad (2)$$

$$\frac{\left(T_{mpv}-T_{ipv}\right)}{R_{pv}/2}-h_{pvac}\left(T_{ipv}-T_{ac}\right)-h_r\left(T_{ipv}^4-T_{ew}^4\right)=0 \quad (3)$$

$$M_{air}\cdot Cp_{air}\cdot\frac{\partial T_{ac}}{\partial t}=h_{pvac}\left(T_{ipv}-T_{ac}\right)+h_{pvac}\left(T_{ew}-T_{ac}\right)+\dot{m}\cdot Cp_{air}\left(T_{inlet}-T_{outlet}\right) \quad (4)$$

$$h_r\left(T_{ipv}^4-T_{ew}^4\right)-h_{wac}\left(T_{ac}-T_{ew}\right)-\frac{\left(T_{ew}-T_{mw}\right)}{R_{pv}/2}=0 \quad (5)$$

$$M_w\cdot Cp_w\cdot\frac{\partial T_{mw}}{\partial t}=\frac{\left(T_{ew}-T_{mw}\right)}{R_{pv}/2}-\frac{\left(T_{mw}-T_{iw}\right)}{R_{pv}/2} \quad (6)$$

$$\frac{\left(T_{mw}-T_{iw}\right)}{R_w/2}-h_i\left(T_{iw}-T_{in}\right)=0 \quad (7)$$

It was considered Tout and Tin as typical Lisbon data temperatures for outdoor and indoor respectively.

3.1.2. BIPV/T-PCM Model

The PCM proprieties used for this simulation are the same as used by Athienitis in [4].
The BIPV/T-PCM system has an equal thermal network at the PV module and at the air cavity. Equations (1) to (5), and (7) are equal for both systems. Equation (6) is replaced by:

$$M_w\cdot Cp_w\cdot\frac{\partial T_{mw}}{\partial t}=\frac{\left(T_{ew}-T_{mw}\right)}{R_{pv}/2}-\frac{\left(T_{mw}-T_{iw}\right)}{R_{pv}/2}+q_l \quad (8)$$

where

$$q_l=2\cdot L_P\cdot R\cdot\frac{T-T_1}{\left(T_1-T_2\right)^2} \quad (9)$$

And

$$L_P=0.62\cdot L \quad (10)$$

q_l is the latent heat flux when phase change occurs [W], L represents the latent heat for complete phase transition (30700 J/Kg), L_p is the latent heat for the temperature range T_1 to T_2 [J/kg], R is the heating or cooling rate [ºC/s], T_1 and T_2 are the temperatures at which the freezing process starts (16ºC) and ends (20.8ºC), respectively [ºC].

3.1.3. Considered parameters

The exterior convective heat transfer coefficient (h_e) used was a Test [5], correlation that takes in count the wind velocity:

$$h_e=8.55+2.56V_{wind} \quad (11)$$

An interior convective heat transfer coefficient (h_{pvac} and h_{wac}) correlation used by Candanedo [6] for inside air cavity was used for both side of the air cavity:

$$h_{pvac}=h_{wac}=8{,}38V_{ch}+1.7635 \quad (12)$$

For the interior room convective heat transfer coefficient (h_i) was considered the one used by Santos [7] as reference value for the horizontal heat flow:

$$h_{pvac}=1/0.13 \qquad \left[W/m^2\cdot{}^\circ C\right] \quad (13)$$

The radiative heat transfer coefficient (h_r) was considered assuming a view factor ($F_{Rpv\text{-}pcm}$) of 1 between planes [8].

$$h_r=\frac{F_{R_{pv-pcm}}\cdot\sigma}{\frac{1}{\varepsilon_{pv}}+\frac{1}{\varepsilon_{pcm}}-1} \quad (14)$$

The sky temperature employed to calculate the radiative heat losses to the exterior is obtained with the following formula [9].

$$T_{sky} = T_e \cdot \left(0.711 + 0.0056 \cdot T_{dp} + 0.000073 \cdot T_{dp}^2 + 0.0013 \cos(\pi) \cdot \frac{1}{12} \right) \quad (15)$$

To calculate the thermal efficiency it was considered a quotient between the gains into the room and the solar radiation (G) times the area of the control volume (Acv). In ventilated cases the gain into the room are considered to be the heat flow through the wall (Qint) plus the air flow (QV) coming from air cavity to the interior room. In non-ventilated cases the gain into the room are simply the heat flow (Qint) through the wall.

Ventilated case:

$$\eta = \frac{Q_{\text{int}} + Q_V}{Q_G \cdot A} \quad (16)$$

Non-ventilated case:

$$\eta = \frac{Q_{\text{int}}}{Q_G \cdot A} \quad (17)$$

4. RESULTS

First of all the numerical model BIPV-T has been validated with experimental results. In the Fig. 5 are presented the results of one day in which respect the temperature inside the air gap Tpv2 and the inlet and outlet corresponding to lower and upper interior vents.

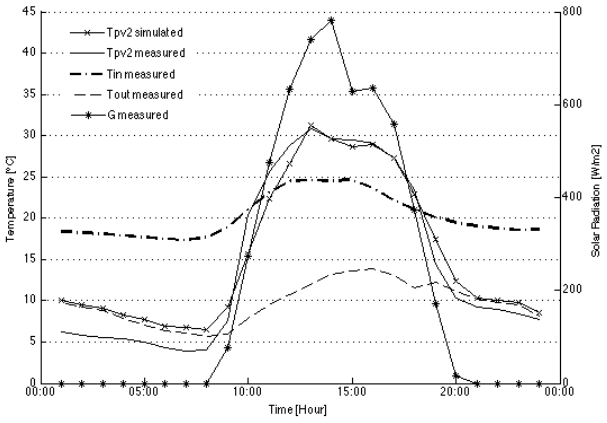

Fig. 5. Validated BIPV-T simulation

As the model has been validated, the model has been modified by substituting the internal layer (brick insulated wall) by PCM gypsum board. The results are presented dor the case of non-ventilated and ventilated air gap. In Fig.6 representative simulation results for the non-ventilated system are presented regarding temperatures of the air inside the cavity. The temperature of the BIPV/T-PCM air reduced to 34ºC as compared to the 43ºC for the BIPV/T. As can be seen, the air temperature of the BIPV-T system is significantly higher than the maximum temperature of the air in the BIPV/T-PCM system (9ºC). This is due to the storage of solar gains as latent heat in the PCM wall. This storage represents a temperature decrease of 21% in air cavity.

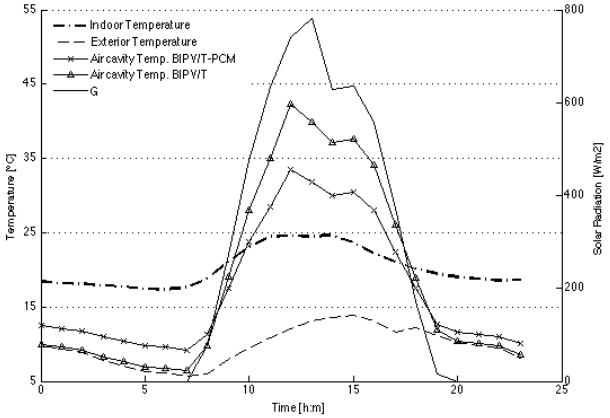

Fig. 6. Simulated air cavity temperature of a non-ventilated BIPV/T and BIPV/T-PCM systems.

Fig. 7 shows the results for the ventilated simulation. In this case the difference between the two systems is lower. The maximum temperature of the air inside the cavity on the BIPV/T is 30 ºC whereas for the BIPV/T-PCM the maximum temperature is 28ºC. This reduction represents a decrease of 7% of the temperature in air cavity. When ventilated, the systems only differ slightly (2ºC). Contrary to what happens in the non-ventilated simulation, the heat produced by the PV overheating, is not stored in PCM as latent heat, but removed by the ventilation system into the room.

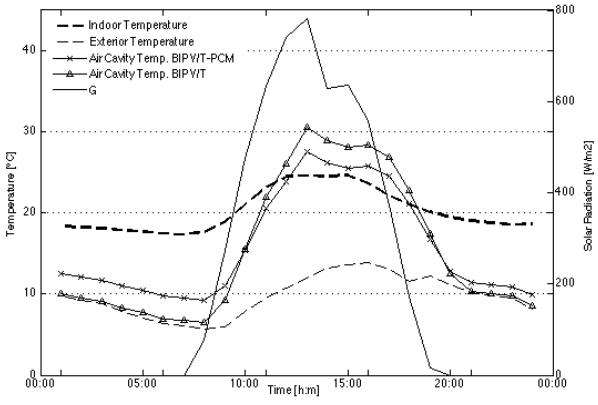

Fig. 7. Simulated air cavity temperature of a ventilated BIPV/T and BIPV/T-PCM systems.

The consequences of the storage of solar gains as latent heat in the PCM wall are felt in the PV temperature. The Fig. 8 shows the PV temperature results for the non-ventilated system simulation. As can be seen, the temperature of the photovoltaic module in the BIPV/T-PCM system is lower than in the BIPV/T system (7ºC). As mentioned above, elevated operating temperatures reduce the solar energy conversion efficiency of photovoltaic module. In this case, the effect of the storage in

PCM reduces the PV temperature and thus raises the PV efficiency. Fig. 8 also shows the interior superficial temperature of the wall. Although the room temperature is defined, a difference between the two different surfaces is evident. The maximum temperature of the surface wall for the BIPV/T is 22ºC and for the BIPV/T-PCM is 19.5ºC. This means that the system with PCM has a surface wall temperature 11% lower. In this case, this is a disadvantage for this system in winter season. The storage of energy in the PCM wall reduces the heat transfer from air cavity to the interior room.

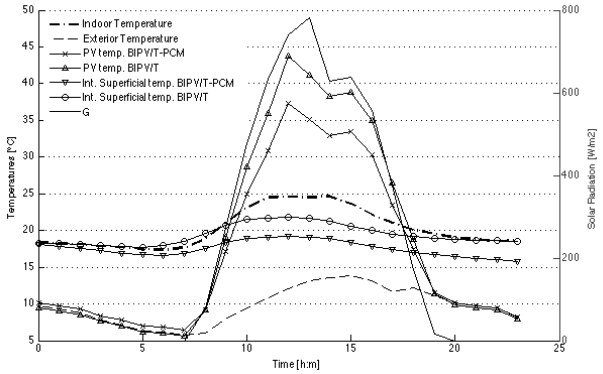

Fig. 8. Simulated PV and Interior superficial temperature of non-ventilated BIPV/T and BIPV/T-PCM systems.

Also, the results in Fig. 8, show, when ventilated, the two systems simulation results for the PV temperature are close (2ºC). As already mentioned, the heat produced by the PV overheating is removed by the ventilation system into the room, and consequently the effect of the storage in PCM almost not feels. On the other hand, the ventilation seems to be positive for PV module. In the case of BIPV/T system, the PV temperature decreased from 44 ºC to 37 ºC. This 7 ºC reduction increases the PV efficiency. Also here, the Fig. 8 shows the interior superficial temperature of the internal layer (wall). The ventilation does not seem to affect the surface temperature. The cause for this is at the interior room defined temperature. Fig. 9 compares the efficiency of ventilated BIPV/T system with non-ventilated BIPV/T-PCM system.

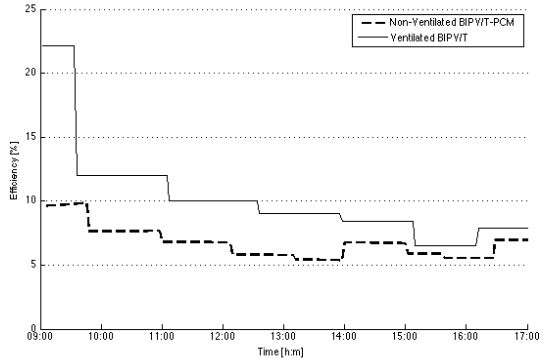

Fig. 8. Ventilated, and non-ventilated BIPV/T and BIPV/T-PCM system efficiency

As can be seen, after a few hours, the efficiency of non-ventilated system with PCM is near the ventilated BIPV/T efficiency. PCM flattens the peaks temperature and makes it more stable, and consequently the efficiency curve is lower but more invariable.

5. CONCLUSIONS

The present study was focused on the numerical thermal analysis of two different systems for integrating on the building façade. The presented results show that the system using PCM decreases the temperature inside the air cavity and make the system more stable due to the storage of solar gains as latent heat in the PCM wall. This is an advantage for the solar energy conversion efficiency of photovoltaic module.

For other hand, the thermal efficiency of the ventilated BIPV/T is higher than the ventilated BIPV/T-PCM due to the airflow at elevated temperature into the room. However, after a few hours, the two systems efficiencies appear to be close to each other. That makes the PCM a reasonable option.

ACKNOWLEDGMENT

This work is part of a project PTDC/AURAQI-AQI/117782/2010 co-financed by FEDER.

REFERENCES

1. P. Office, Directive 2010/31/EU of the European Parliament and of the Council of 19 May 2010 on the energy performance of buildings. 2010, p. 13-35.

2. Y. Chen, A. K. Athienitis, and K. Galal, “Modeling, design and thermal performance of a BIPV/T system thermally coupled with a ventilated concrete slab in a low energy solar house: Part 1, BIPV/T system and house energy concept,” Solar Energy, vol. 84, no. 11, p. 1892-1907, Nov. 2010.

3. A. Bouzoukas, New Approaches for cooling photovoltaic/thermal (PV/T) Systems, Nottingham: University of Nottingham, 2008.

4. A. K. Athientis, C. Liu, D. Hawes, D. Banu, and D. Feldman, “Investigation of the thermal performance of a passive solar test-room with wall latent heat storage,” Building and Environment, vol. 32, no. 5, p. 405-410, Dec. 1997.

5. F. L. Test, R. C. Lessmann, and A. Johary, “Heat Transfer During Wind Flow over Rectangular Bodies in the Natural Environment,” Journal of Heat Transfer, vol. 103, no. 2, p. 262-267, Jan. 1981.

6. L. Candanedo, A. K. Athienitis, L. O'Brien, and J. Candanedo, “Transient and Steady State Models for Open-Loop Air-Based BIPV/T Systems ,” ASHRAE Transactions,, p. 1-24, Jan. 2010.

7. C. A. P. D. Santos and L. M. C. Matias, Coeficientes De Transmissão Térmica De Elementos Da Envolvente Dos Edíficios, 1st ed., vol. 1. Lisboa: LNEC, 2006, p. 1-171.

8. S. A. Kalogirou, Solar Energy Enginnering, 1st ed. London: Elsivier, 2009, p. 1-757.

9. A. J. Duffie and A. W. Beckman, Solar Engineering, 2nd ed. Jonh Wiley & Sons, INC, 1980, p. 1-470.